

A Qubit as a Bridge Between Statistical Mechanics and Quantum Dynamics

Manmeet Kaur* and Somendra M. Bhattacharjee†

Department of Physics, Ashoka University, Sonapat, Haryana - 131029, India

(Dated: June 23, 2025)

This work presents a unified perspective on thermal equilibrium and quantum dynamics by examining the simplest quantum system, a qubit, as a foundational model. We show that both the thermal partition function and the Loschmidt amplitude can be understood as extensions of a single analytic function along different paths in the complex plane. The zeros of Loschmidt amplitude encode dynamical features such as orthogonality, rate function singularities, and quantum speed limits, in analogy with the role of partition function zeros in equilibrium statistical mechanics. We further establish, through the Cauchy-Riemann equations, that the high-temperature specific heat corresponds to early-time evolution. The discussion follows a pedagogical progression from a single qubit to an interacting spin chain.

Key words: Quantum spin models, Quantum quench, Lee-Yang and Fisher zeroes.

I. INTRODUCTION

The boundary between thermal physics and quantum dynamics is often drawn sharply; the former is related to equilibrium ensembles, while the latter describes unitary time evolution. Yet at a fundamental level, both frameworks aim to understand how physical systems access and evolve through their available states. In this work, we investigate how a single quantum system, *a qubit*, representing a two-level system [1], can reveal a connection between these two domains.

In statistical mechanics, the partition function captures how a system's microscopic configurations contribute to its macroscopic thermodynamic properties in equilibrium. In contrast, the Loschmidt amplitude plays a central role in quantum dynamics and information theory, measuring the overlap between an evolving quantum state and its initial configuration. Despite their different contexts, we show that both quantities can be written as extensions of a single analytic function in the complex plane.

To develop this connection, we begin with a single qubit. We observe that both the partition function and the Loschmidt amplitude can be expressed as a polynomial in a complex variable y , whose roots encode unifying features of thermal and dynamical behavior. While the model lacks true phase transitions, the zeros still reflect important signatures such as bounds imposed by quantum speed limits and logarithmic divergences in the rate functions. The framework is then generalised to many-body systems, including a chain of non-interacting qubits and an interacting spin system. Throughout, we take a pedagogical approach, highlighting how basic models can illuminate the analytic structure underlying both equilibrium and nonequilibrium quantum physics.

A. Outline

This paper is organized as follows. [Section II](#) introduces the central model and describes the physical setup. While [Section III](#) discusses the thermal description of the qubit using the canonical partition function, [Section IV](#) turns to the quantum dynamics of the same system at zero temperature. We compute the Loschmidt amplitude, and identify special times when the system becomes orthogonal to its initial state. [Section V](#) develops an analytic framework that brings together thermal and quantum descriptions and [Section VI](#) extends this framework to many-body settings. Starting with a chain of N non-interacting qubits, we move towards interactions by considering an interacting spin chain with open boundary conditions. [Section VII](#) concludes with reflections on the significance of the unifying analytic framework as well as its pedagogical potential. [Appendix A](#) discusses Mandelstam–Tamm and Margolus–Levitin bounds for our specific models.

II. THE TWO-LEVEL SYSTEM: SETUP

Let us consider a qubit with two non-degenerate energy levels. The Hamiltonian lives in a two-dimensional Hilbert space, with the energy spectrum given by

$$H|0\rangle = -J|0\rangle, \quad H|1\rangle = 0|1\rangle \quad (1)$$

where $|0\rangle$ and $|1\rangle$ form an orthonormal basis of energy eigenstates, see [Fig. 1](#). This defines the simplest non-trivial quantum system. In quantum information, this system naturally serves as a qubit, the basic unit of quantum computation. Another physical realization is a spin- $\frac{1}{2}$ particle in a magnetic field, where the energy levels correspond to spin-up and spin-down along the field axis.

arXiv:2506.15931v1 [quant-ph] 19 Jun 2025

* manmeet.kaur.phd20@ashoka.edu.in

† somendra.bhattacharjee@ashoka.edu.in

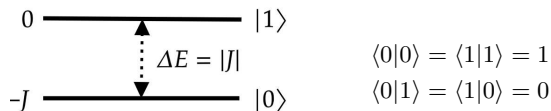


FIG. 1. A schematic diagram of a qubit's energy levels with an energy gap ΔE of magnitude $J(> 0)$ between the two levels. On the right, the orthonormality conditions of the basis states are shown.

III. THERMAL DESCRIPTION: QUANTUM STATISTICAL MECHANICS

The thermodynamic properties of the qubit, coupled to a heat bath at inverse temperature $\beta = 1/(k_B T)$, where T is the temperature and k_B is the Boltzmann constant, are governed by the partition function

$$Z(y) = \frac{1}{2} \sum_{\alpha=0}^1 e^{-\beta E_\alpha} = \frac{1}{2}(1+y), \quad y = e^{\beta J}, \quad (2)$$

with $E_0 = -J$ and $E_1 = 0$ as defined in Eq. (1). The prefactor $\frac{1}{2}$ helps in subtracting the entropy of the high-temperature limit. For positive temperatures, the physically relevant regime in this work, the parameter y lies in the range $[1, \infty)$.

Including the negative temperatures, a regime associated with population inversion in certain systems [2], the domain of y extends to the interval $(0, \infty)$.

Importantly, for all real values of β , the function $Z(y)$ remains analytic and strictly positive.

IV. QUANTUM DESCRIPTION: UNITARY TIME EVOLUTION

In contrast to the thermal description, where the qubit is in contact with a heat bath, we now examine the dynamics of the same qubit, but in isolation and at zero temperature. With the energy conserved, its time evolution is governed by the unitary operator $U(t) = e^{-iHt/\hbar}$ (\hbar being the reduced Planck constant).

Initially, we prepare the qubit in the superposition state

$$|\psi(0)\rangle = \frac{1}{\sqrt{2}}(|0\rangle + |1\rangle), \quad (3)$$

which is clearly not an energy eigenstate of the Hamiltonian, and it evolves in time as

$$|\psi(t)\rangle = e^{-iHt/\hbar}|\psi(0)\rangle = \frac{1}{\sqrt{2}}(y|0\rangle + |1\rangle), \quad y = e^{iJt/\hbar}. \quad (4)$$

Here $y = e^{iJt/\hbar}$ is the natural analytic continuation of the variable defined in Eq. (2). This *complex Boltzmann factor* traverses a unit circle as $t \in (-\infty, \infty)$ [3] in the complex- y plane, see Fig. 2. The unitary evolution introduces a relative phase between the energy eigenstates, though the individual state probabilities remain constant,

$$P_\alpha(t) = |\langle \alpha | \psi(t) \rangle|^2 = \frac{1}{2}, \quad \alpha = 0, 1. \quad (5)$$

For the dynamical behavior, we examine the Loschmidt amplitude, the overlap between the initial and time-evolved states

$$L(y) = \langle \psi(0) | \psi(t) \rangle = \frac{1}{2} \sum_{\alpha} e^{iE_\alpha t} = \frac{1}{2}(1+y). \quad (6)$$

This overlap determines how distinguishable the time-evolved state is from the initial one, when $L(y) = 0$, the states are orthogonal and perfectly distinguishable.

The return probability (also known as the *Loschmidt echo*) provides the likelihood of the system to return to its initial state after a time t and is given by,

$$P(y) = |L(y)|^2. \quad (7)$$

This quantity oscillates in time, and the qubit returns to its initial state periodically, see Inset B, Fig. 3. These oscillations are analogous to Rabi cycles seen in two-level systems under resonant driving, though here they arise purely from free evolution. The return probability vanishes when $\cos(Jt) = -1$, at

$$t_c = \frac{(2n+1)\pi\hbar}{J}, \quad n \in \mathbb{Z}. \quad (8)$$

At these special times, the system reaches a state orthogonal to the initial one, a physically distinguishable configuration. The minimum time required to reach an orthogonal state (in proper units) is thus given by

$$t_\perp = \frac{\pi\hbar}{J}, \quad (n=0). \quad (9)$$

The quantum speed bounds proposed by Mandelstam–Tamm and Margolus–Levitin are saturated in this case [4, 5]. For a discussion of these limits in the context of a qubit, see appendix A.

V. A UNIFIED FRAMEWORK: PARTITION FUNCTION AND LOSCHMIDT AMPLITUDE

A connection between thermal and quantum descriptions of the qubit arises when we observe that both the partition function (Eq. 2) and the Loschmidt amplitude (Eq. 6) share a common algebraic structure. We define a dynamical partition function $\mathcal{L}(y)$ via analytic continuation, using y as a complex variable,

$$\mathcal{L}(y) = \frac{1}{2}(1+y) = \begin{cases} Z(y), & y = e^{\beta J}, \quad y \in \mathbb{R}^+ \\ L(y), & y = e^{iJt/\hbar}, \quad |y| = 1. \end{cases} \quad (10)$$

This unified polynomial structure allows us to interpret the Loschmidt amplitude and the partition function as two manifestations of a single analytic object, differing only in the path traversed in the complex- y plane. Just as the partition function yields the (dimensionless) thermal free energy,

$$f_{\text{thermal}}(y) \sim -\ln Z(y), \quad (11)$$

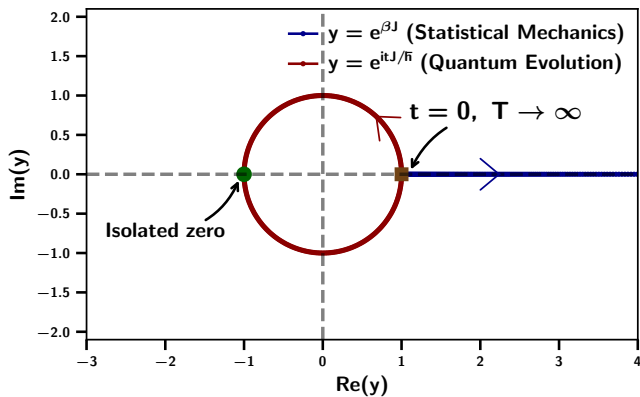


FIG. 2. The blue line represents the real Boltzmann factor from statistical mechanics, which never intersects the isolated zero at $y = -1$ (the green point). The red unit circle corresponds to quantum time evolution. It traces the imaginary Boltzmann factor, periodically crossing the zero. The brown square at $y = 1$ marks both the infinite-temperature limit $\beta \rightarrow 0$ and the initial time of the quantum system $t \rightarrow 0$.

we define a free energy-like quantity, which we refer to as the dynamical free energy,

$$f_{\text{dyn}}(y) \sim -\ln \mathcal{L}(y). \quad (12)$$

It is a complex-valued function, with its real part

$$f_L(y) = \text{Re}(f_{\text{dyn}}(y)), \quad (13)$$

determining the return probability via

$$P(y) = \exp[-2f_L(y)]. \quad (14)$$

The key parallels between thermodynamics and quantum dynamics for a qubit are summarized in Table I.

A. High-Temperature Limit and Early-Time Expansion: Cauchy-Riemann Equations

We now analyze the behavior of $\mathcal{L}(y)$ in the vicinity of $y = 1$, which corresponds to the infinite-temperature limit in the thermal case and the initial time in the quantum evolution. In the thermal regime, the second derivative of the free energy determines the specific heat,

$$C(\beta) = -k_B \beta^2 \frac{d^2 f_{\text{thermal}}}{d\beta^2}. \quad (15)$$

This gives specific heat at high-temperatures as,

$$C(\beta) \underset{\text{high } T}{\approx} -\frac{k_B}{8} J^2 \beta^2. \quad (16)$$

Since $f_{\text{dyn}}(y)$ is analytic in a neighborhood of $y = 1$, see Eq. (10) and Eq. (12), the Cauchy-Riemann conditions apply and allow us to expand the dynamical free energy $f_{\text{dyn}}(y)$ in a Taylor series around $y = 1$. These conditions guarantee that the complex derivatives are independent

of the directions along which the point is approached. We choose two orthogonal directions: (i) along the real axis and (ii) along the tangent to the unit circle $y = 1$. These correspond, respectively, to high-temperature expansion in β and early-time expansion in t , see Fig. 2. As a result, just as the high-temperature specific heat reflects energy fluctuations, the same information appears in the coefficient of the t^2 term in the Taylor expansion of $f_L(y)$. This analytic equivalence illustrates how early-time evolution in the quantum regime mirrors high-temperature thermodynamic behavior, see Table I. In particular, for early times i.e. $\frac{Jt}{\hbar} \ll 1$, this correspondence gives us

$$f_L(t) \approx C(\beta) \Big|_{\beta \rightarrow it/\hbar} \underset{\text{small } t}{\approx} \frac{1}{8\hbar^2} J^2 t^2, \quad (17)$$

where the second approximation follows from Eq.(15) and Eq.(16). The quadratic behavior in t near $t = 0$ is shown as Inset A, Fig. 3.

Quantity	Thermal Case	Quantum Case
Variable	$y = e^{\beta J} \in \mathbb{R}^+$	$y = e^{iJt}, y = 1$
Function	$Z(y) = \frac{1}{2}(1+y)$	$L(y) = \frac{1}{2}(1+y)$
Free energy	$f_{\text{thermal}}(y) \sim -\ln Z(y)$	$f_{\text{dyn}}(y) \sim -\ln L(y)$
Free energy behavior	Continuous and finite	May exhibit logarithmic divergences
Physical observable	$Z(y) \sim e^{-f_{\text{thermal}}}$	$P(y) \sim e^{-2f_L(y)}$
Energy fluctuation near $y = 1$	$-\beta^2 \frac{d^2 f_{\text{thermal}}}{d\beta^2} \Big _{y=1}$	$t^2 \frac{d^2 f_L}{dt^2} \Big _{y=1}$
Interpretation	High-temperature specific heat	Early-time unitary evolution

TABLE I. Comparison of thermal and quantum formulations in a two-level system, highlighting the role of the analytic function $\mathcal{L}(y)$ and its implications. The correspondence between fluctuation terms links high-temperature thermodynamics and short-time quantum dynamics near $y = 1$.

B. Zeros and Divergences

For the qubit, $\mathcal{L}(y)$ has a single isolated zero at

$$y_0 = -1, \quad (18)$$

as seen from Eq. (10). The importance of zeros of the partition function was originally explored in the context of phase transitions by Lee, Yang, and Fisher [2], where the limit points of complex zeros on the real axis signal singularities in the thermodynamic limit. In general, the behavior of a polynomial is governed by the location of its zeros. In the thermal case, where $y = e^{\beta E} \in \mathbb{R}^+$, the zero at $y = -1$ lies outside the physical domain and remains inaccessible. In contrast, in the quantum case, whenever the evolution path crosses the zero at $y = -1$,

$f_L(y)$ diverges logarithmically, as shown in Fig. 2 and Fig. 3. This indicates that in unitary dynamics, the system becomes orthogonal to its initial state, causing the return probability to vanish and the real dynamical free energy to diverge.

The possibility of crossing zero depends on the system's energy spectrum. For example, in a degenerate two-level system, such as when the excited state $E_1 = 0$ as defined in Eq. (1), is two-fold degenerate; the zero lies off the unit circle, and the return probability remains nonzero at all times. That is, the system never evolves into a state orthogonal to its initial configuration.

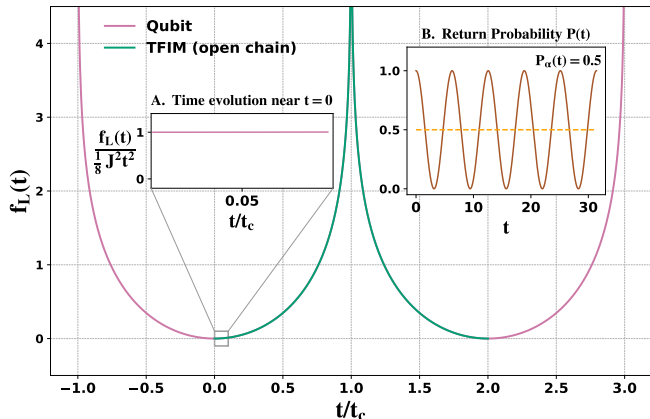


FIG. 3. Periodic logarithmic divergences are observed in the real dynamical free energy $f_L(y)$ as a function of scaled time in (i) a qubit and (ii) TFIM with open boundary conditions. Inset A. Early evolution of a system is shown to have a quadratic dependence in time for small t , (17). Inset B. The system periodically “forgets” ($P(t) = 0$) and “remembers” ($P(t) = 1$) its initial state due to unitary evolution. The probabilities $P_0(t)$ and $P_1(t)$ remain constant throughout.

A side note. This framework also invites an electrostatic analogy, especially natural in two dimensions. The zero of $\mathcal{L}(y)$ at $y = -1$ can be viewed as the location of a point charge in the complex- y plane, and the dynamical free energy $f_{\text{dyn}}(y)$, plays the role of the electrostatic potential generated by this charge. While this analogy is not particularly useful for the qubit system discussed here, it becomes a powerful tool in understanding phase transitions in more complex many-body systems.

VI. EXTENSION TO MANY-BODY SYSTEMS

We now examine the collective behavior of a many-body system under two complementary approaches: thermal equilibrium (when the system is connected to a heat bath) and unitary quantum dynamics (when the system is isolated). To this end, we consider a chain of N non-interacting qubits, living in a 2^N -dimensional Hilbert space.

In the thermal setting, the additivity of the Hamiltonian implies that the total partition function factorizes

as

$$Z_N(y) = [Z(y)]^N = \left(\frac{1+y}{2}\right)^N, \quad (19)$$

where $Z(y)$ is the single-qubit partition function defined earlier in Eq. (2), and Z_N is the partition function of the full N -qubit chain. The free energy per qubit in the thermodynamic limit is then given by

$$f_{\text{thermal}}(y) = \lim_{N \rightarrow \infty} -\frac{1}{N} \ln Z_N(y) = -\ln\left(\frac{1+y}{2}\right). \quad (20)$$

On the quantum side, we consider an initial product state of the form

$$|\Psi(0)\rangle = \prod_{j=1}^N |\psi_j(0)\rangle, \quad (21)$$

where each $|\psi_j(0)\rangle$ is the initial state of qubit j as defined in Eq. (3). Under unitary evolution with a non-interacting Hamiltonian, the state at time t becomes

$$|\Psi(t)\rangle = \prod_{j=1}^N (e^{-iHt/\hbar} |\psi_j(0)\rangle). \quad (22)$$

The corresponding Loschmidt amplitude for the many-body system is the product of single-qubit amplitudes,

$$\mathcal{L}_N(y) = [\mathcal{L}(y)]^N, \quad (23)$$

where $\mathcal{L}(y)$ is the amplitude associated with a single qubit, as defined in Eq. (10) and $\mathcal{L}_N(y)$ denotes the Loschmidt amplitude of the full system. Following the single-qubit case, we define a quantum analog of the free energy density per qubit in the thermodynamic limit:

$$f_{\text{dyn}}(y) \equiv \lim_{N \rightarrow \infty} -\frac{1}{N} \ln \mathcal{L}_N(y) = -\ln \mathcal{L}(y). \quad (24)$$

The physical observables are then given by, see Eq. (13) and Eq. (14),

$$f_L(y) = \text{Re}(f_{\text{dyn}}(y)), \quad (25)$$

and the return probability in the large- N limit becomes

$$P(y) = \exp[-2N f_L(y)]. \quad (26)$$

The exponential form of Eq. (26) plays a central role in large deviation theory [6], where the probabilities of rare fluctuations decay exponentially with system size, as $P(t) \sim \exp[-NI(t)]$, where $I(t)$ is known as the rate function, defined in the large- N limit as

$$I(t) = \lim_{N \rightarrow \infty} -\frac{1}{N} \ln P(t). \quad (27)$$

In our context, we identify $I(t) = f_L(y)$, which captures the fact that the probability of observing a trajectory that deviates significantly from typical quantum evolution is exponentially suppressed in N .

The behavior of the real dynamical free energy density in this non-interacting case is identical to that of the single-qubit system. By bridging thermal and quantum perspectives, this connection enables techniques developed for computing free energies in thermal systems to be adapted, via analytic continuation, to study dynamical properties of time-evolving quantum systems through their associated rate functions.

A. Toward Interactions

We now examine how the analytic structure discussed above extends to systems with interactions. Specifically, we consider a one-dimensional chain of N spin- $\frac{1}{2}$ particles with open boundary conditions, defined in a 2^N -dimensional Hilbert space.

Each site i hosts a spin described by the Pauli operators $\sigma_i^x, \sigma_i^y, \sigma_i^z$. In this section, we focus on an interaction Hamiltonian involving only the σ^z operators:

$$H = -\frac{J}{2} \sum_{i=1}^{N-1} \sigma_i^z \sigma_{i+1}^z, \quad (28)$$

where $J/2$ sets the nearest-neighbor interaction strength. The Pauli matrices are given by

$$\sigma^x = \begin{pmatrix} 0 & 1 \\ 1 & 0 \end{pmatrix}, \quad \sigma^y = \begin{pmatrix} 0 & -i \\ i & 0 \end{pmatrix}, \quad \sigma^z = \begin{pmatrix} 1 & 0 \\ 0 & -1 \end{pmatrix}.$$

This Hamiltonian is diagonal in the basis of product eigenstates of the σ_i^z operators. Since each spin can take eigenvalues ± 1 , the Hilbert space consists of 2^N distinct configurations of the form $\{s_1, s_2, \dots, s_N\}$, where $s_i = \pm 1$ is the eigenvalue of σ_i^z at site i . The states $|\uparrow\rangle$ and $|\downarrow\rangle$ refer to the eigenstates of σ^z with eigenvalues $+1$ and -1 , respectively. A configuration is thus a sequence of N such eigenstates. The corresponding energy eigenvalue of the chain is

$$E = -\frac{J}{2} \sum_{i=1}^{N-1} s_i s_{i+1}, \quad (29)$$

which is precisely the *classical* Ising model.

In the thermal setting, the partition function is

$$Z_N = \text{Tr} e^{-\beta H} = \sum_{\{s_i = \pm 1\}} e^{\beta \frac{J}{2} \sum_{i=1}^{N-1} s_i s_{i+1}}. \quad (30)$$

To simplify this sum, we introduce bond variables $\zeta_i = s_i s_{i+1} \in \{\pm 1\}$, so that the energy becomes

$$E = -\frac{J}{2} \sum_{i=1}^{N-1} \zeta_i. \quad (31)$$

To simplify the spectrum, we shift this energy expression by a constant, which does not affect the physics, as

$$E = -J \sum_{i=1}^{N-1} \left(\frac{1 + \zeta_i}{2} \right), \quad (32)$$

so that the two energy levels per bond are illustrated in Fig. 1. The minimal excitation corresponds to flipping a bond, giving an energy gap $\Delta E = J$. Because the bond variables are independent, the partition function factorizes across bonds. This leads to [7]

$$Z_N(y) = \left(\frac{1+y}{2} \right)^{N-1}. \quad (33)$$

This reproduces the same polynomial form as in the non-interacting case with $N-1$ such zeros lying at $y = -1$, still being outside the thermal domain.

We now turn to the quantum dynamics of the same model. The system is initially prepared in a product state that is not an eigenstate of the Hamiltonian. One such choice is the ground state of a strong transverse field, which aligns all spins along the \hat{x} -direction. At $t = 0$, the transverse field is quenched to zero, and the system evolves under the Ising interaction described in Eq. (28). The corresponding initial state

$$|\Psi(0)\rangle = \prod_{j=1}^N |\psi_j(0)\rangle, \quad |\psi_j(0)\rangle = \frac{1}{\sqrt{2}} (|\uparrow_j\rangle + |\downarrow_j\rangle), \quad (34)$$

is not an eigenstate of the Hamiltonian, ensuring non-trivial dynamics.

The Loschmidt amplitude can be computed as the overlap between the initial state and the time-evolved state. Using Eq.(32), this leads to

$$\mathcal{L}(y) = \frac{1}{2^N} \sum_{\{s_j = \pm 1\}} e^{iEt/\hbar} = \left(\frac{1+y}{2} \right)^{N-1}. \quad (35)$$

This expression shares the same analytic structure as the thermal partition function and exhibits a zero at $y = -1$. Thus, under certain interactions and boundary conditions, the rate function governing the collective behavior of the system retains the same features as observed in the single-qubit case.

VII. CONCLUSION

The central idea unifying the thermal and dynamical descriptions is that both the partition function and the Loschmidt amplitude can be expressed as evaluations of a single analytic function $\mathcal{L}(y)$ along different paths in the complex y -plane. In thermal physics, $y = e^{\beta E}$ lies on the positive real axis, while in quantum dynamics, $y = e^{iEt/\hbar}$ traces the unit circle. This analytic continuation shows that dynamical features such as orthogonality and singularities in dynamical free energy are governed by the same underlying zero structure that also encodes thermal properties.

The qubit-based approach presented here is both accessible and rigorous, and thus can easily be incorporated in a statistical mechanics or a quantum mechanics course. This framework opens a pedagogical entry point for introducing advanced concepts such as dynamical quantum

phase transitions, large deviation theory, and more complex phenomena in interacting systems using only familiar tools from undergraduate physics. Such advanced topics can further be assigned as projects to the students. As the connection between equilibrium and nonequilibrium physics continues to unfold, the deceptively simple qubit serves as a reminder that deep insights often emerge from minimal models.

Acknowledgements MK thanks Axis Bank for their financial support.

Appendix A: Quantum Speed Limits (QSLs)

At a fundamental level, quantum mechanics imposes a natural constraint on how fast a qubit, or more generally any quantum system, can evolve in time. In particular, there exists a minimum (*first*) time required for a system to evolve from an initial state to one that is orthogonal to it. This *orthogonalization time*, denoted by τ_{\perp} , is defined by the condition $\langle \psi_0 | \psi(\tau_{\perp}) \rangle = 0$.

In our qubit model, this time is found to be

$$\tau_{\perp} = \frac{\pi\hbar}{J}, \quad (\text{A1})$$

as discussed in Eq. (9) in the main text.

Quantum speed limits (QSLs) place lower bounds on τ_{\perp} . These bounds arise from the spectral properties of the Hamiltonian and the system's energy distribution in the initial state. Two key bounds [4] are commonly used,

- **Mandelstam–Tamm (MT) bound:**

This bound is determined by the energy uncertainty ΔE , defined as $\Delta E = \sqrt{\langle H^2 \rangle - \langle H \rangle^2}$. It gives

$$\tau_{\perp} \geq \tau_{\text{MT}} = \frac{\pi\hbar}{2\Delta E}. \quad (\text{A2})$$

- **Margolus–Levitin (ML) bound:**

This bound uses the average energy above the ground state. Assuming the spectrum is shifted so that $\varepsilon_n = E_n - E_0$, the average shifted energy is $\langle \varepsilon \rangle = \langle H \rangle - E_0$, and the bound takes the form

$$\tau_{\perp} \geq \tau_{\text{ML}} = \frac{\pi\hbar}{2\langle \varepsilon \rangle}. \quad (\text{A3})$$

Since both bounds are valid and independent, the tightest constraint on the orthogonalization time is given by

$$\tau_{\perp} \geq \max(\tau_{\text{MT}}, \tau_{\text{ML}}) = \max\left(\frac{\pi\hbar}{2\Delta E}, \frac{\pi\hbar}{2\langle \varepsilon \rangle}\right). \quad (\text{A4})$$

Both bounds vanish in the classical limit $\hbar \rightarrow 0$, as expected. We now derive each bound and evaluate them explicitly for the qubit.

1. Mandelstam–Tamm Bound

We begin with the uncertainty relation between two Hermitian operators A and B :

$$\Delta A \Delta B \geq \frac{1}{2} |\langle [A, B] \rangle|. \quad (\text{A5})$$

Taking $B = H$ and using the Heisenberg equation $[A, H] = -i\hbar \frac{dA}{dt}$, we obtain

$$\Delta A \Delta H \geq \frac{\hbar}{2} \left| \frac{d}{dt} \langle A \rangle \right|. \quad (\text{A6})$$

Choosing $A = |\psi_0\rangle\langle\psi_0|$, the projection operator onto the system's initial state, the return probability $P(t) = |\langle\psi_0|\psi(t)\rangle|^2$ corresponds to the expectation value of A in the time-evolved state. The variance of A is then given by $P(1 - P)$. Substituting into Eq. (A6) gives

$$\Delta H \geq \frac{\hbar}{2} \frac{1}{\sqrt{P(1 - P)}} \left| \frac{dP}{dt} \right|. \quad (\text{A7})$$

Integrating over time up to τ_{\perp} , where $P(\tau_{\perp}) = 0$, we find

$$\tau_{\perp} \geq \frac{\hbar}{2\Delta H} \int_1^0 \frac{dP}{\sqrt{P(1 - P)}} = \frac{\pi\hbar}{2\Delta H} = \tau_{\text{MT}}. \quad (\text{A8})$$

For the qubit initialized in the *cat* state (Eq. 3) and evolving under the Hamiltonian in Eq. 1, the energy variance is

$$(\Delta H)^2 = \langle \psi_0 | H^2 | \psi_0 \rangle - \langle \psi_0 | H | \psi_0 \rangle^2 = \frac{J^2}{4}, \quad (\text{A9})$$

which gives $\Delta H = J/2$, independent of time. Substituting into Eq. (A8) provides

$$\tau_{\text{MT}} = \frac{\pi\hbar}{J}, \quad (\text{A10})$$

in agreement with the exact orthogonalization time τ_{\perp} in Eq. (A1).

2. Margolus–Levitin Bound

Let $H|n\rangle = E_n|n\rangle$, and consider the initial pure state

$$|\psi(0)\rangle = \sum_n c_n |n\rangle, \quad \sum_n |c_n|^2 = 1, \quad (\text{A11})$$

with shifted energies $\varepsilon_n = E_n - E_0$. Under time evolution, the state becomes

$$|\psi(t)\rangle = \sum_n c_n e^{-i\varepsilon_n t/\hbar} |n\rangle. \quad (\text{A12})$$

The Loschmidt amplitude is

$$L(t) = \langle \psi(0) | \psi(t) \rangle = \sum_n |c_n|^2 e^{-i\varepsilon_n t/\hbar}. \quad (\text{A13})$$

Taking the real part and applying the inequality $\cos \theta \geq 1 - \frac{2}{\pi}\theta - \frac{2}{\pi}\sin \theta$, for $0 \leq \theta \leq \pi$, we obtain

$$\operatorname{Re} L(t) \geq 1 - \frac{2t}{\pi\hbar} \langle \varepsilon \rangle - \frac{2}{\pi} \operatorname{Im} L(t), \quad (\text{A14})$$

with

$$\langle \varepsilon \rangle = \sum_n |c_n|^2 \varepsilon_n = \langle H \rangle - E_0. \quad (\text{A15})$$

At $t = \tau_\perp$, the amplitude vanishes and both its real and imaginary parts are identically zero, implying

$$0 \geq 1 - \frac{2\tau_\perp}{\pi\hbar} \langle \varepsilon \rangle, \quad (\text{A16})$$

which leads to the ML bound

$$\tau_\perp \geq \frac{\pi\hbar}{2\langle \varepsilon \rangle} = \tau_{\text{ML}}. \quad (\text{A17})$$

In our qubit model (see, Eqs. 1, 3 and A12), we have

$$\langle \varepsilon \rangle = \frac{1}{2}J, \quad (\text{A18})$$

so that

$$\tau_{\text{ML}} = \frac{\pi\hbar}{J}, \quad (\text{A19})$$

which again coincides with τ_\perp , indicating that the Margolus–Levitin bound is also saturated in this model.

3. Scaling of QSLs in Many-Body Systems

In Sec. VI, we consider a non-interacting qubit chain and an interacting spin chain with bond-variable representation. In both cases, the total Hamiltonian is additive over N effective degrees of freedom (qubits or bonds). Consequently, the average energy $\langle E \rangle$ scales linearly with N , while the energy uncertainty ΔE grows as \sqrt{N} for independent product states. Substituting into the QSL bounds in Eqs. (A2) and (A3), we find that $\tau_{\text{ML}} \sim 1/N$ and $\tau_{\text{MT}} \sim 1/\sqrt{N}$. For $N \rightarrow \infty$, both the bounds vanish and therefore *do not* provide much information about the QSLs.

-
- [1] J. Preskill, “Lecture Notes for Physics 229: Quantum Information and Computation,” California Institute of Technology, Chapter 2, 2015. https://www.preskill.caltech.edu/ph219/chap2_15.pdf
- [2] R. K. Pathria and P. D. Beale, *Statistical Mechanics*, 3rd ed., Elsevier (2011).
- [3] The negative time reflects the time-reversal symmetry of the Schrödinger equation governing unitary evolution.
- [4] M. Frey, “Quantum speed limits—primer, perspectives, and potential future directions,” *Quantum Inf Process*, **15**, 3919 (2016). [doi:10.1007/s11128-016-1405-x](https://doi.org/10.1007/s11128-016-1405-x).
- [5] S. Deffner and S. Campbell, “Quantum speed limits: from Heisenberg’s uncertainty principle to optimal quantum control,” *J. Phys. A: Math. Theor.* **50** 453001 (2017). [doi:10.1088/1751-8121/aa86c6](https://doi.org/10.1088/1751-8121/aa86c6).
- [6] H. Touchette, “The large deviation approach to statistical mechanics,” *Phys. Rep.* **478**, 1 (2009). [doi:10.1016/j.physrep.2009.05.002](https://doi.org/10.1016/j.physrep.2009.05.002).
- [7] In the non-interacting case, each of the N qubits contributes independently. In the interacting case, only $N - 1$ bonds contribute due to open boundaries.